

Manifestation of anharmonicities in terms of Fano scattering and phonon lifetime of scissors modes in α -MoO₃

Ravindra Kumar Nitharwal,^a Vivek Kumar,^b Anubhab Sahoo,^a M. S. Ramachandra Rao,^{a,c} Tejendra Dixit,^{d*} and Sivarama Krishnan^{a,c*}

^aDepartment of Physics, Indian Institute of Technology, Madras, Chennai-600036, E-mail: srkrishnan@iitm.ac.in

^bDepartment of Physics, Indian Institute of Information Technology Design and Manufacturing, Kancheepuram, Chennai-600127, India

^cQuantum Center of Excellence for Diamond and Emergent Materials (QuCenDiEM)

group, Indian Institute of Technology, Madras, Chennai -600036, India

^dOptoelectronics and Quantum Device Group, Department of Electronics and Communication Engineering, Indian Institute of Information Technology Design and Manufacturing, Kancheepuram, Chennai-600127, India; E-mail: tdixit@iiitdm.ac.in

Table of contents

Fig. S1: EDX of the α -MoO₃.

Fig. S2: Normalized temperature-dependent Raman spectrum of α -MoO₃ (633 nm excitation).

Table 1: The calculated coupling coefficient and asymmetry ratio of scissors modes at various temperatures (633 nm excitation).

Fig. S3: Temperature-dependent PL spectra of α -MoO₃ (488 nm excitation).

Fig. S4: Temperature-dependent Raman spectra of α -MoO₃ (488 nm excitation).

Fig. S5: Fano-Raman line-shape fitted plot of scissors modes (488 nm excitation).

Fig S6: Variation of coupling coefficient and asymmetry ratio with temperature (488 nm excitation).

Table 2: The calculated coupling coefficient and asymmetry ratio values for scissors modes at different temperatures (488 nm excitation).

Table 3: Extracted parameters from the Fano-Raman line-shape fitting of 818 cm^{-1} stretching mode at 633 nm excitation.

Fig. S7: Anharmonic variation in the frequency and linewidth of 818 cm^{-1} (A_g) stretching mode (633 nm excitation wavelength).

Fig S8: Variation in the Phonon lifetime of 818 cm^{-1} (A_g) stretching mode (633 nm excitation wavelength).

Table 4: Extracted parameters from the anharmonic model fitting of 818 cm^{-1} (A_g) mode.

Table 5: The shift in phonon frequency in conjunction with the rate of change in frequency resulting from temperature.

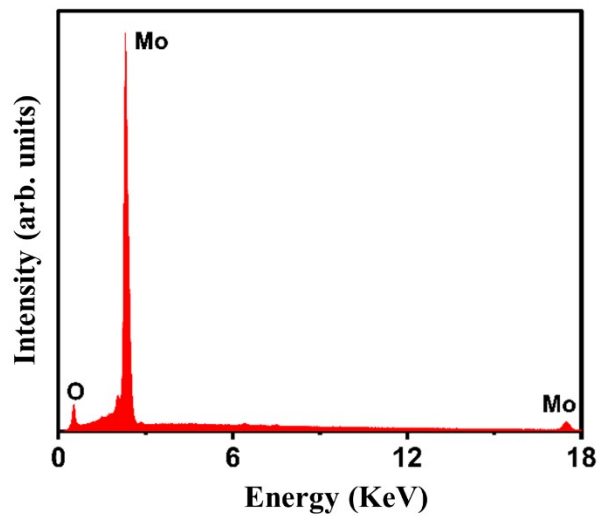


Fig. S1. EDX profile of α -MoO₃ confirms that oxygen and molybdenum elements are present in the pellet.

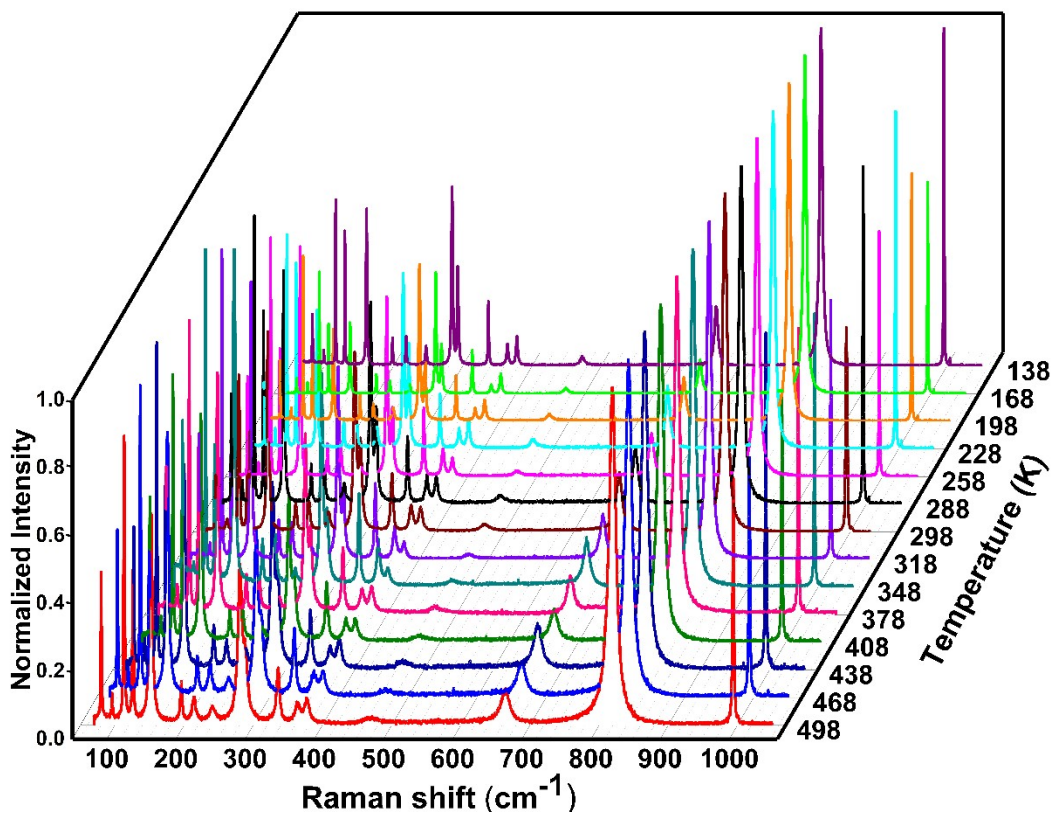


Fig. S2. Normalized temperature-dependent Raman spectrum of α -MoO₃ pellet recorded using 633 nm laser excitation.

Table 1. Obtained coupling coefficient values from fitting of both scissors modes with Fano-Raman line-shape function and corresponding asymmetry ratio at 633 nm excitation wavelength.

Temperature (K)	$A_g(1)$ mode		$B_{1g}(1)$ mode	
	Coupling coefficient (1/q)	Asymmetry ratio ($\alpha_R = \Gamma_L / \Gamma_H$)	Coupling coefficient (1/q)	Asymmetry ratio ($\alpha_R = \Gamma_L / \Gamma_H$)
138	0.050	1.00	-0.017	1.01
168	0.080	0.96	-0.014	1.00
198	0.081	0.95	-0.030	1.05
228	0.083	0.94	-0.028	1.02
258	0.143	0.88	-0.056	1.10
288	0.099	0.93	-0.036	1.08
298	0.117	0.92	-0.118	1.19
318	0.132	0.90	-0.087	1.15
348	0.159	0.87	-0.094	1.16
378	0.164	0.84	-0.108	1.18
408	0.208	0.78	-0.164	1.28
438	0.263	0.75	-0.153	1.20
468	0.385	0.70	-0.218	1.35
498	0.313	0.73	-0.192	1.30

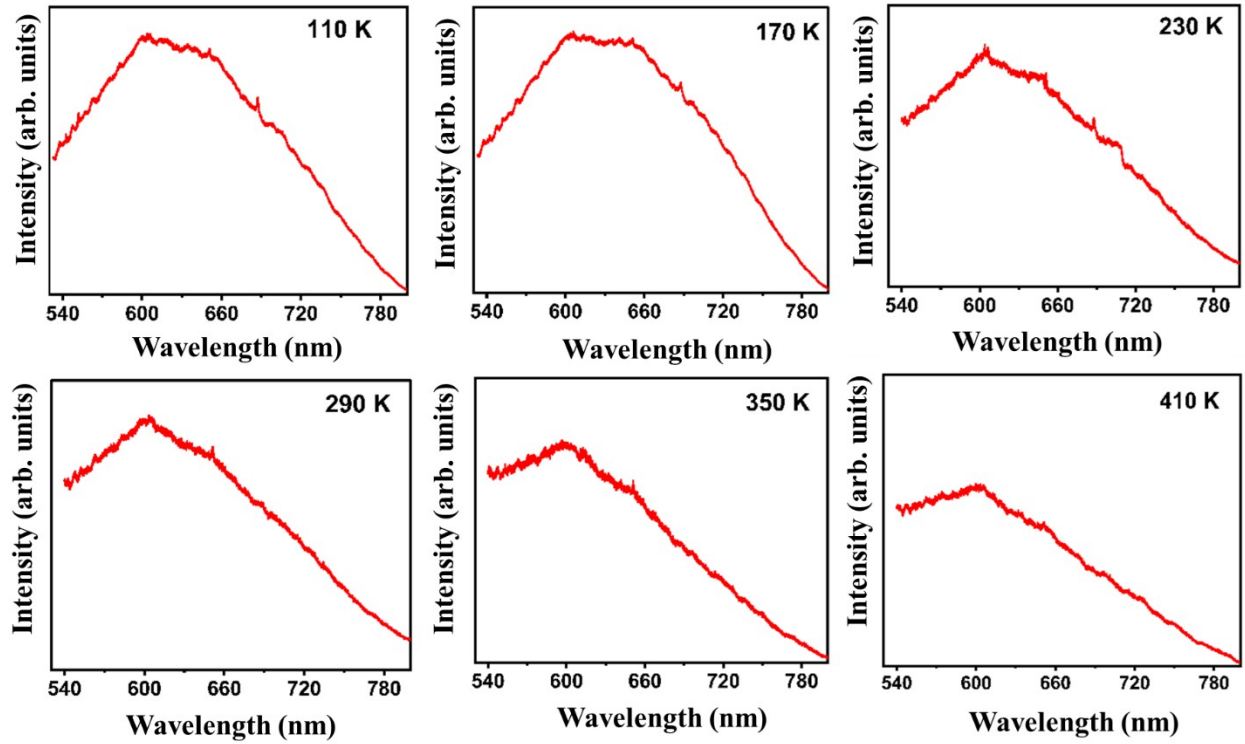


Fig. S3. Temperature-dependent PL spectra α - MoO_3 at 488 nm laser excitation and observation of more energy continuum at higher temperatures.

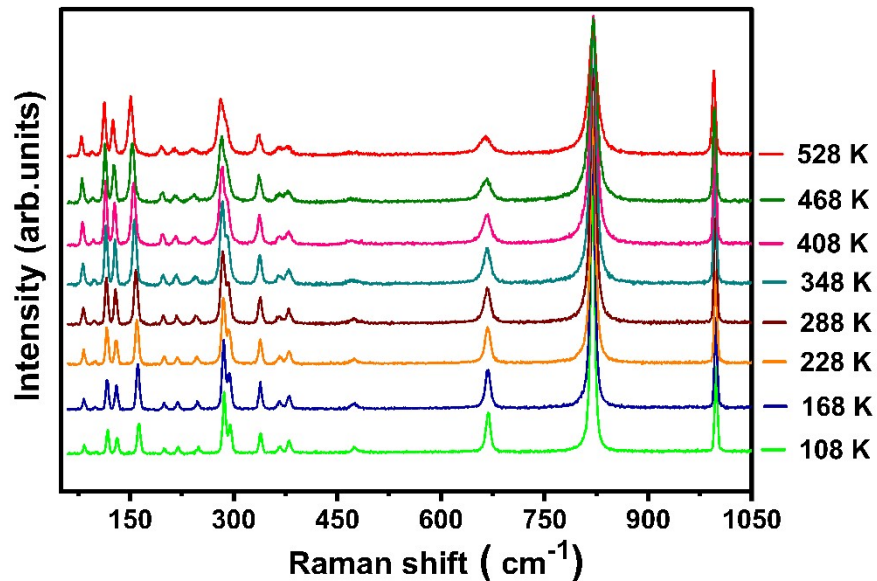


Fig. S4. Representative temperature dependence Raman spectra of α -MoO₃ pellet recorded using 488 nm laser excitation.

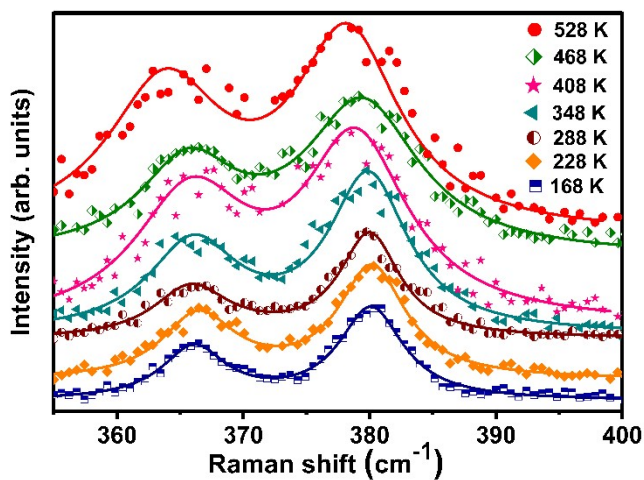


Fig. S5. Temperature-dependent asymmetric behavior of $A_g(1)$ and $B_{1g}(1)$ scissor modes at 488 nm laser excitation. Here, different colored lines represent the theoretical fitting at different temperatures using the Fano-Raman line-shape function.

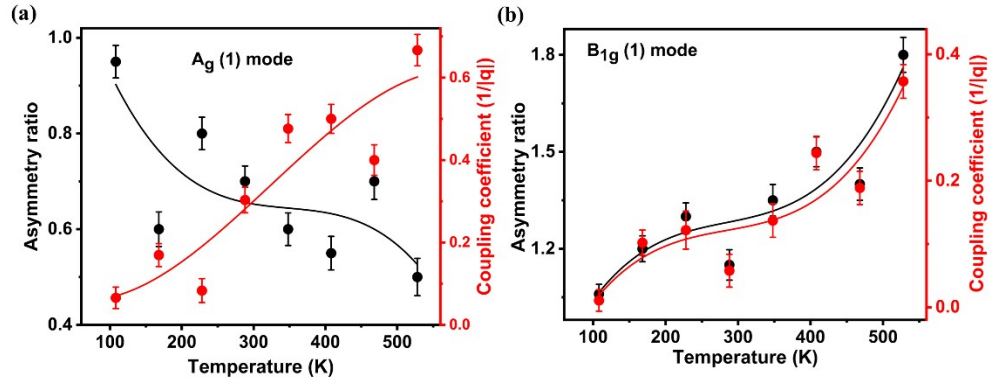


Fig. S6. Panels (a) and (b) show the variation in the asymmetry ratio (left y-axis) and coupling coefficient (right y-axis) with temperature for $A_g(1)$ and $B_{1g}(1)$ scissor modes at 488 nm excitation wavelength, respectively. The error bar represents the uncertainties in calculated fitting parameters.

Table 2. Coupling coefficient obtained by fitting of both scissor modes with the Fano-Raman line-shape function and corresponding asymmetry ratio at 488 nm excitation wavelength.

Temperature (K)	$A_g(1)$ mode		$B_{1g}(1)$ mode	
	Coupling coefficient (1/q)	Asymmetry ratio ($\alpha_{R= \Gamma_L / \Gamma_H}$)	Coupling coefficient (1/q)	Asymmetry ratio ($\alpha_{R= \Gamma_L / \Gamma_H}$)
108	0.065	0.95	-0.010	1.06
168	0.169	0.62	-0.102	1.20
228	0.083	0.80	-0.121	1.30
288	0.303	0.66	-0.057	1.15
348	0.476	0.60	-0.137	1.35
408	0.500	0.55	-0.237	1.50
468	0.400	0.70	-0.188	1.40
528	0.660	0.50	-0.357	1.80

Table 3. Obtained coupling coefficient by the fitting of 818 cm^{-1} stretching mode with the Fano-Raman line-shape function and corresponding asymmetry ratio for a few temperatures at 488 nm and 633 nm excitation wavelengths.

Temperature (K)	488 nm		633 nm	
	Coupling coefficient ($1/q$)	Asymmetry ratio ($\alpha_{R=\Gamma_L/\Gamma_H}$)	Coupling coefficient ($1/q$)	Asymmetry ratio ($\alpha_{R=\Gamma_L/\Gamma_H}$)
168	0.00051	1.004	0.00053	1.002
228	0.00015	1.000	0.00014	1.000
288	0.00060	1.005	0.00055	1.003
348	0.00054	1.003	0.00034	1.001
408	0.00064	1.006	0.00036	1.002
468	0.00087	1.008	0.00054	1.005

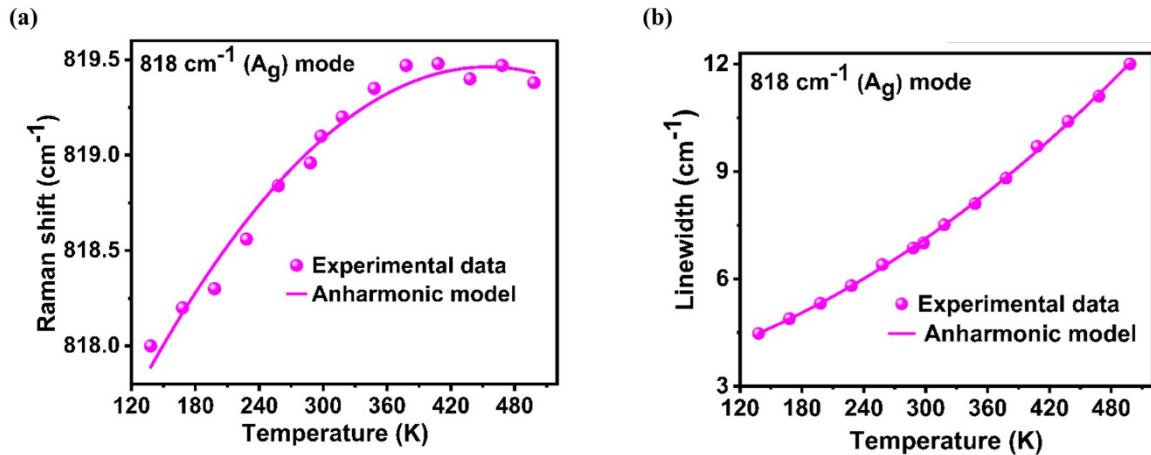


Fig. S7. (a) and (b) represent the temperature dependency of the 818 cm^{-1} stretching mode's frequency and linewidth, respectively. The pink spheres refer to experimental data, and the solid pink line indicates the fitting of temperature-dependent frequency and linewidth using an anharmonic model at 633 nm excitation.

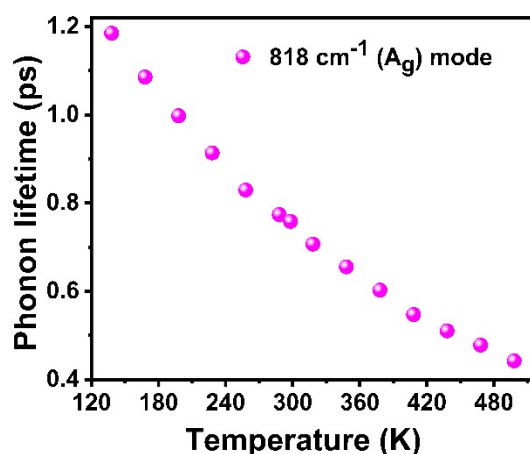


Fig. S8. Variation in the phonon lifetime of 818 cm^{-1} stretching mode with temperature at 633 nm excitation wavelength.

Table 4. Extracted parameters from the fitting of the 818 cm^{-1} (A_g) stretching mode by the

Anharmonic parameters	Extracted value
A	0.014 ± 0.001
B	$-1.57 \times 10^{-4} \pm 0.18 \times 10^{-4}$
C	$0.061 \pm 0.95 \times 10^{-5}$
D	$2.32 \times 10^{-4} \pm 0.15 \times 10^{-4}$

Anharmonic model.

Table 5. The extent of variation in phonon frequency in relation to the rate of change of frequency driven by temperature.

Raman mode	Position at 138 K (cm^{-1})	Position at 498 K (cm^{-1})	$\frac{d\omega}{dT}$ (cm^{-1}/K)	Total shift (cm^{-1})
$A_g(1)$	365.1	362.65	0.007	-2.45
$B_{1g}(1)$	378.25	377.2	0.003	-1.05
A_g	818	819.4	0.004	1.4

